

Permanent Magnet Synchronous Machine Parameters Identification for Load Characteristics Calculation

DOI 10.7305/automatika.2015.07.813
UDK 621.313.32:621.313.8; 621.317

Original scientific paper

Self reactance X_d in direct axis 'd' and self reactance X_q in quadrature axis 'q' influence the load characteristics of the permanent magnet machine. Their calculation methods are known. All calculations should be verified by measurements. Measurement with AC variable voltage and frequency source applied on stator winding is correct when eddy currents do not exist. Other methods evaluate the DC current decay after initial direct current was applied on the stator winding. Accuracy of these methods is lowered because of the numerical evaluation of current decay curve. Another method performs the measurement on the machine loaded as a motor. The load angle β is measured by a machine set of four machines. The accuracy is lowered by higher harmonics induced in no load in the helping synchronous machine. The load angle can be also obtained by geometrical construction of the vector diagram. In this paper the evaluation of the generator steady state regime of the machine is used. The generator works with different loads consisting of capacitance, inductance or arbitrary impedance or resistance. When the generator transfers from no load to load regime the rotor is shifting and the load angle changes. This angle is measured. The newly proposed measurement methods are simple in special cases of loads. Results of measurements and their experimental verification are published in the paper.

Key words: Electric machines, Parameter identification, Permanent magnet machinery, Synchronous machines, Variable speed drive

Identifikacija parametara sinkronog stroja s permanentnim magnetima za proračun karakteristika opterećenja. Reaktancija X_d u uzdužnoj 'd' osi i reaktancija X_q u poprečnoj 'q' osi utječu na karakteristike opterećenja stroja s permanentnim magnetima. Metode za njihov izračun su poznate. Svaki izračun trebao bi se potvrditi mjerenjima. Mjerenje korištenjem izmjeničnog izvora s promjenjivim naponom i frekvencijom priključenim na statorske namote prikladno je kada nema vrtložnih struja. Druge metode procjenjuju opadanje istosmjernje struje nakon što je prethodno narinuta struja u uzdužnoj osi. Točnost ovih metoda umanjena je zbog numeričke evaluacije krivulje opadanja struje. Također se koristi i metoda koja vrši mjerenja na opterećenom stroju u motornom režimu rada. Kut opterećenja β mjeri se korištenjem skupa od četiri stroja. Točnost je smanjena zbog induciranih viših harmonika u praznom hodu zbog pomoćnog sinkronog stroja. Kut opterećenja može se također dobiti geometrijskim pristupom iz faznog dijagrama. U ovom radu korištena je procjena u stacionarnom stanju uz generatorski režim rada. Generator je opterećen različitim trošilima koja uključuju kapacitivno, induktivno, otporno ili s proizvoljnom impedancijom. Prijelaznu pojavu generatora iz praznog hoda u opterećeni režim rada prati promjena rotorskih veličina i kuta opterećenja. Ovaj kut je moguće izmjeriti. Predložena metoda mjerenja jednostavna je uz posebne vrste opterećenja. U radu su prikazani rezultati mjerenja uz eksperimentalnu potvrdu metode.

Ključne riječi: Električni strojevi, identifikacija parametara, stroj s permanentnim magnetima, sinkroni stroj, elektromotorni pogon promjenjive brzine

1 INTRODUCTION

Progress in power electronic converters brought radical change of synchronous machine usage area. They operated with constant frequency usually [1,2]. Synchronous machines supplied by electronic converters are first of all widely used as permanent magnet synchronous machine (PMSM) in variable speed drives [3–8]. New application

field lies also in electric vehicle drives [9] and aircraft [10]. Permanent magnet synchronous machines have influenced the usage of electronic converters on the other hand too [11–13].

Synchronous machine usage area caused construction modifications according to different technologies and areas where machines are used. Other changes in construction

were caused by permanent magnet development [14]. Self reactance X_d and X_q depend not only on machine construction but also on the permanent magnet material quality. Classical salient-pole synchronous machines with rotor winding for field current have $X_d > X_q$ and their ratio is usually

$$\frac{X_d}{X_q} \in (1.3; 2.5).$$

This proportion changes in PMSM sharply. Many PMSM have X_d and X_q nearly the same. But indispensable number of PMSM has the ratio

$$\frac{X_d}{X_q} \in (0.5; 1.5).$$

That means that $X_d < X_q$ is also possible [8, 11, 15–17]. The calculation methods of direct axis reactance X_d and quadrature axis reactance X_q are known. Also the finite element method is possible. All calculations surely contain uncertainty caused by nonlinear iron features, geometrical complexity, permanent magnet material features and by accepted presumptions [18]. That means calculations should be verified by experiments any case. Reactances of variable speed PMSM are usually expressed as inductances for practical reasons. There were used different measurement methods for direct axis inductance L_d and quadrature axis inductance L_q in literature. In [19] two methods are used. The first method is using an AC-source with variable voltage and frequency applied on stator winding for synchronous inductances measurement. The rotor must be fixed in the phase axis on which the direct inductance L_d is measured and then shifted 90° electrical degrees for L_q measurement. The method is correct when in the machine eddy currents do not exist. The second method, described also in [20], evaluates the DC current decay after initial direct current was applied. In [15] a similar voltage step method was used. Accuracy of these methods is lowered because of the numerical evaluation of the current time curve. Current decay can last several minutes in turboalternators as mentioned in [20]. Paper [3] uses the steady state working when the machine is loaded as a motor. Under this condition the magnetic fluxes in 'dq' axes are constant. The torque angle (load angle) β is measured by a machine set of four machines. The accuracy is lowered by higher harmonics induced in no load in the helping synchronous machine. Paper [17] uses also the steady state analysis. The load angle is obtained by geometrical construction which lowers the accuracy too.

2 MEASUREMENT OF PMSM PARAMETERS IN STEADY-STATE CONDITION

The newly proposed measurement methods are described in this section. They are simple and accurate. They

can be used also for machines where eddy currents in the 'dq' axes exist and cannot be omitted.

In this paper the evaluation of steady state of the machine working as generator is used. The generator is loaded with capacitance or inductance when L_d inductance is measured. The generator is loaded with arbitrary impedance or resistance when L_q inductance is measured. This load causes that the torque angle (load angle) β occurs. When the machine transfers from no load to load regime the rotor is shifting and the torque angle changes from zero to β . This angle can be measured by the position sensor or by the stroboscope. The vector diagram in steady state is depicted in Fig. 1. The angle β is the angle between stator voltage U_1 and voltage U_b induced by permanent magnet flux.

To construct the diagram following values must be known:

R_1 stator resistance

X_d stator self reactance in 'd' axis

X_q stator self reactance in 'q' axis

U_1 stator voltage

I_1 stator current

φ phase angle.

2.1 Measurement of stator self inductance in 'd' axis

Vector diagram in Fig. 1 will change when the PMSM is loaded as generator by capacitance or inductance only. For the case of the capacitance load see Fig. 2.

The stator current vector $I_1 = I_C$ is situated in the direct axis 'd' as its magnetic flux linkage $\Psi_c = L_d \cdot I_1$. Voltage U_b is induced by the permanent magnet flux.

The magnetic flux linkage $\Psi_c = L_d \cdot I_1$ will be added to the magnetic flux linkage of the permanent magnet which induces the voltage U_b . It holds exactly when R_1 is zero or very small. For the case of inductance load the magnetic flux linkage Ψ will be subtracted from the magnetic flux linkage of the permanent magnet. The direct axis inductance is the function of the magnetic circuit and permanent magnet quality. We can measure the voltage U_b of the PMSM in no load. The direct axis reactance $X_{1d} + X_{1\sigma}$ can be calculated from the difference of no load voltage and load voltage. It holds when we omit the resistance R_1 . The voltage drop on the resistance R_1 is small when compared with the stator voltage U_1 . The calculation can be corrected with respect to the voltage drop $R_1 \cdot I_C$. The correction is usually not needed. The vector diagram is shown in Fig. 2 for the case when the machine was loaded with capacitance. Voltage drop $R_1 \cdot I_C$ is assumed as very low.

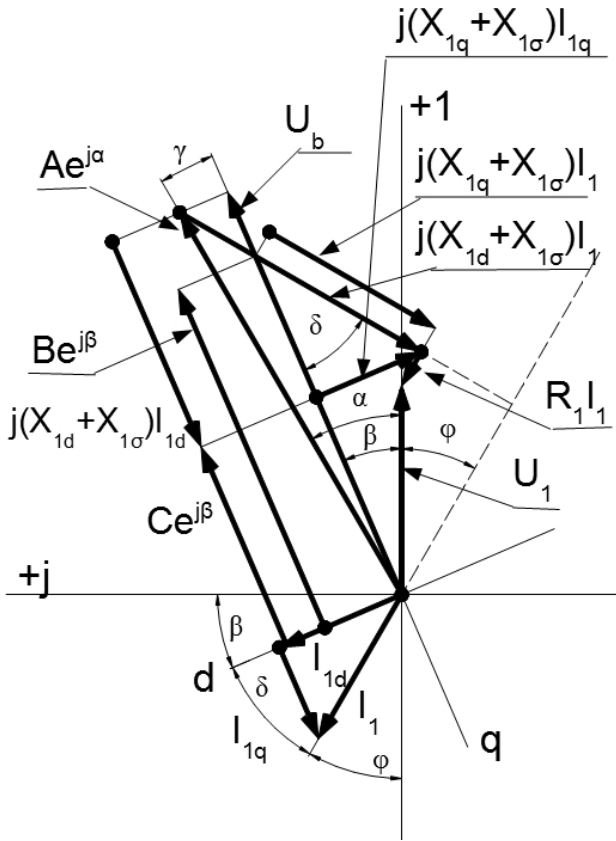


Fig. 1. Vector diagram of salient pole synchronous machine loaded by inductance in steady state generator regime, $X_d > X_q$

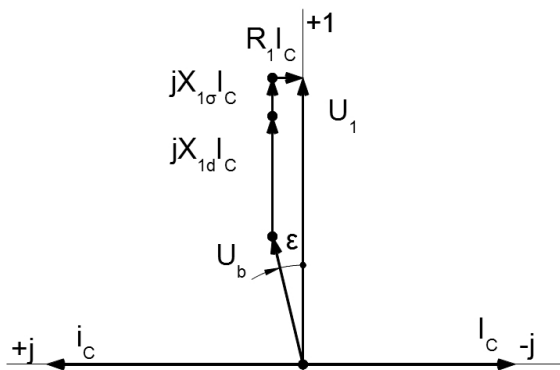


Fig. 2. Vector diagram of PMSM loaded by capacitance. Voltage vector U_1 was laid into the real axis.

We can calculate:

$$X_{1d} + X_{1\sigma} = \frac{U_1 - U_b \cdot \cos \varepsilon}{I_c}, \quad (1)$$

$$L_{1d} + L_{1\sigma} = \frac{X_{1d} + X_{1\sigma}}{\omega}. \quad (2)$$

It holds for the angle ε :

$$\sin \varepsilon = \frac{R_1 \cdot I_c}{U_b}. \quad (3)$$

For $R_1 \cdot I_c = 10 \text{ V}$ and $U_b = 220 \text{ V}$, $\varepsilon \approx 2.60^\circ$ and $\cos \varepsilon = 0.9989$.

The correction is not necessary even if it is possible.

We can calculate the time constant knowing the stator phase resistance $R_1 = R_d$.

$$T_d = \frac{L_{1d} + L_{1\sigma}}{R_d}, \quad (4)$$

$$T_d = \frac{U_1 - U_b \cdot \cos \varepsilon}{R_d \cdot \omega \cdot I_c}. \quad (5)$$

Procedure is the same when we load the machine with inductance.

2.2 Measurement of stator self inductance in 'q' axis

Measurement may be performed on the machine loaded as generator. The load can be arbitrary combination of resistance, inductance and capacitance.

Directly measurable values are:

$R_1 = R_d$ stator phase resistance

U_1 stator voltage

U_b voltage induced by the permanent magnet in no load regime

Z loading impedance

φ phase angle

$L_d = L_{1d} + L_{1\sigma}$ Direct axis inductance is known from previous measurement

ω electrical angular frequency.

We use for the measurement evaluation the vector diagram in Fig. 3 which is drawn for the case that $L_d < L_q$.

The position and the length of the vector $|A| \cdot e^{j\alpha}$ can be calculated from (6).

$$\vec{A} = \vec{U}_1 - R_1 \cdot \vec{I}_1 - j(X_{1d} + X_{1\sigma}) \cdot \vec{I}_1 = |A| \cdot e^{j\alpha}. \quad (6)$$

The value $L_d = L_{1d} + L_{1\sigma}$ was measured and is known. The length of the vector and its angle α can be calculated from (6). The length of the vector $|B| \cdot e^{j\beta}$ depends on $L_{1q} + L_{1\sigma}$.

$$\vec{B} = \vec{U}_1 - R_1 \cdot \vec{I}_1 - j(X_{1q} + X_{1\sigma}) \cdot \vec{I}_1. \quad (7)$$

$$\begin{aligned}
 &= j \frac{U_1 + R_1 \cdot I_1}{I_{1q}} \cdot (\cos \beta - j \sin \beta - \cos \beta) = \\
 &= \frac{U_1 + R_1 \cdot I_1}{I_1 \cdot \cos \beta} \cdot \sin \beta = \\
 &= \frac{U_1 + R_1 \cdot I_1}{I_1} \cdot \tan \beta. \quad (17)
 \end{aligned}$$

It holds for the stator self reactance in quadrature axis and stator self inductance in quadrature axis simple (18) and (19) finally.

$$X_{1q} + X_{1\sigma} = \frac{U_1 + R_1 \cdot I_1}{I_1} \cdot \tan \beta, \quad (18)$$

$$L_{1q} + L_{1\sigma} = \frac{X_{1q} + X_{1\sigma}}{\omega} = \frac{U_1 + R_1 \cdot I_1}{I_1 \cdot \omega} \cdot \tan \beta. \quad (19)$$

It is only the measurement in the regime of resistance load needed. Only voltage U_1 , current I_1 and angle β between U_1 and U_b are needed. The angle β can be measured by the position sensor or by the stroboscope. Angle β marks the 'dq' axes shifting when the machine rotor transfers from no load to load regime or on the contrary.

3 PERFORMED MEASUREMENTS

Measurements were performed according to the Chapter 2. Measured machine was: Synchronous machine 1 kW, 140 V, star connected, 3 phases, 4.6 A, 133.33 Hz, 2000 min^{-1} , pole number $2p = 8$, with buried permanent magnets symmetrically distributed. Photo of the measured machine is in Fig. 4. Measurement arrangement is in Fig. 5.



Fig. 4. PMSM 1 kW, 140 V, star connected, 3 phases, 4.6 A, 133.33 Hz, 2000 min^{-1} , pole number $2p = 8$, with buried permanent magnets symmetrically distributed

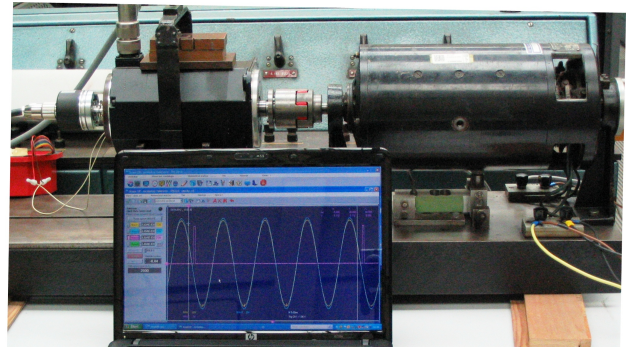


Fig. 5. Measurement arrangement

3.1 Influence of saturation in the machine during measurement

Saturation of the magnetic circuit in PMSM is caused by two factors. The first factor is the permanent magnet in itself and the second factor is the armature reaction caused by load. Permanent magnets have good quality nowadays. Nevertheless the coercive field strength H_c and remanent magnetic flux density B_r are limiting factors for the machine design. Therefore the saturation level of the magnetic circuit at no load is rather low. The influence of the armature reaction on the magnetic saturation in PMSM is lower as in machines using excitation winding. Let us compare it using the magnetic circuit in Fig. 6. The reluctance of the armature stack is assumed to be much smaller than the reluctance of the air gap. Let us consider the case when the armature reaction is zero. It means that the armature coil in Fig. 6 is without current.

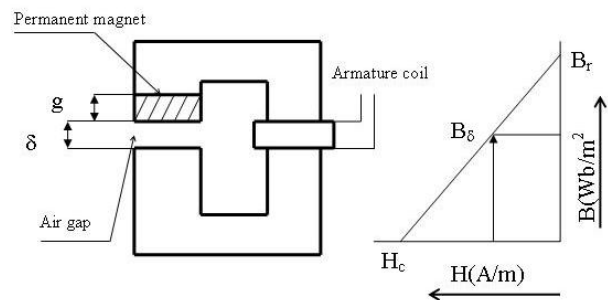


Fig. 6. Magnetic circuit with permanent magnet, armature reaction and the demagnetization curve $H = f(B)$

It holds between the air gap magnetic flux density B_δ , coercive field strength H_c and the remanent magnetic flux density B_r (20).

$$B_\delta = B_r - \frac{B_r \cdot B_\delta}{g \cdot H_c \cdot \mu_0} \cdot \delta, \quad (20)$$

from which we get:

$$B_{\delta} = \frac{B_r}{1 + \frac{B_r \cdot \delta}{g \cdot H_c \cdot \mu_0}} \quad (21)$$

When the armature coil current is present and causes the MMF it will hold:

$$B_{\delta} = B_r - \frac{B_r}{g \cdot H_c} \cdot \left(\frac{B_{\delta}}{\mu_0} \cdot \delta \mp MMF \right), \quad (22)$$

from which we get:

$$B_{\delta} = \frac{B_r \cdot \left(1 \pm \frac{MMF}{g \cdot H_c} \right)}{1 + \frac{B_r \cdot \delta}{g \cdot H_c \cdot \mu_0}} \quad (23)$$

The sign '+' holds in case when the MMF supports the permanent magnet. The sign '-' holds in case when the MMF acts against the permanent magnet.

Let us assume that the magnetic circuit is magnetized only with excitation winding (not depicted in Fig. 6). The permanent magnet is not used and the armature reaction causes additionally the same MMF as in the previous case. The armature reaction MMF causes additional air gap magnetic flux density B_{δ} :

$$\Delta B_{\delta} = \mu_0 \cdot \frac{MMF}{\delta} \quad (24)$$

Let us calculate the increasing of the air gap magnetic flux density ΔB_{δ} caused by armature winding MMF 100 A.

Parameters of the magnetic circuit are listed in Table 1.

The magnetic flux density in the air gap when the circuit is magnetized only by permanent magnet is given by (21) $B_{\delta} = 0.7020$ T.

The magnetic flux density in the air gap when the circuit is magnetized by permanent magnet and by armature reaction with MMF 100 A is given by (23) $B_{\delta} = 0.7207$ T.

The increasing of the magnetic flux density in the air gap is $\Delta B_{\delta} = 0.0187$ T.

The increasing of the magnetic flux density in the air gap when the magnetic circuit is magnetized by excitation winding and additionally by armature reaction

Table 1. Parameters of the magnetic circuit

Length of the permanent magnet	$g = 0.005$ m
Length of the air gap	$\delta = 0.002$ m
Coercive field strength of the permanent magnet	$H_c = 750\,000$ Am ⁻¹
Permanent magnet remanent magnetic flux density	$B_r = 1$ T

with MMF 100 A is given by (24) $\Delta B_{\delta} = 0.0628$ T. That means that the influence of the armature reaction is in machine with excitation winding 3.358 times stronger than in PMSM.

In all these cases were the air gap magnetic flux densities B_{δ} calculated under the assumption that the reluctance of the armature stack is negligible. Nevertheless the results show that the saturation effect can appear in PMSM only at very high loads and is much more weaker than in machines with exciting windings. Approximately similar results hold in 'q' axis because also here the magnetic flux crosses the permanent magnet material. Magnetic flux crosses in this case the side extension parts of permanent magnet poles. Therefore the measured values can be used in prevailing loads. When we want to calculate load characteristics of the machine at high loads it is better to measure the self inductances at high currents but with attention not to demagnetize the permanent magnet.

3.2 Measurement of stator self inductance in 'd' axis.

Machine was loaded with capacitive current.

3.2.1 Values measured

Stator effective phase voltage $U_1 = 58.38$ V, phase voltage induced with permanent magnets $U_b = 55.71$ V. Capacitive current $I_C = 1.117$ A. Frequency during measurement $f = 99.16$ Hz, angular velocity $\omega = 623.04$ s⁻¹, revolutions 1487.4 min⁻¹, phase resistance $R_1 = R_d = 0.963$ Ω.

3.2.2 Results obtained

Using (1) we obtain the reactance X_d at frequency $f = 99.16$ Hz:

$$X_d = X_{1d} + X_{1\sigma} = \frac{U_1 - U_b}{I_c} = \frac{58.38 - 55.71}{1.117} = 2.39 \Omega. \quad (25)$$

Using (2) we get stator self inductance:

$$L_d = L_{1d} + L_{1\sigma} = \frac{X_{1d} + X_{1\sigma}}{\omega} = \frac{2.39}{623.04} = 0.003836 \text{ H}. \quad (26)$$

Using (4) we get the time constant:

$$T_d = \frac{0.003836}{0.963} = 0.003983 \text{ s}. \quad (27)$$

The angle ϵ can be omitted because:

$$\begin{aligned} \sin \epsilon &= \frac{R_d \cdot I_c}{U_b} = \frac{0.963 \cdot 1.117}{55.71} = 0.0193, \\ \epsilon &= 1.106^\circ, \\ \cos \epsilon &= 0.9998. \end{aligned} \quad (28)$$

3.3 Measurement of stator self inductance in 'q' axis.

Machine was loaded with resistance only.

3.3.1 Values measured

Stator effective phase voltage $U_1 = 25.92$ V. Current $I_R = 2.265$ A. Frequency during measurement $f = 52.5$ Hz. Angular velocity $\omega = 329.87$ s⁻¹, revolutions 787.5 min⁻¹. Phase resistance $R_1 = R_d = 0.963$ Ω. Angle $\beta = 8.510^\circ$ was measured with position sensor. Graph of voltage U_b is measured in no-load and is depicted in Fig. 7.

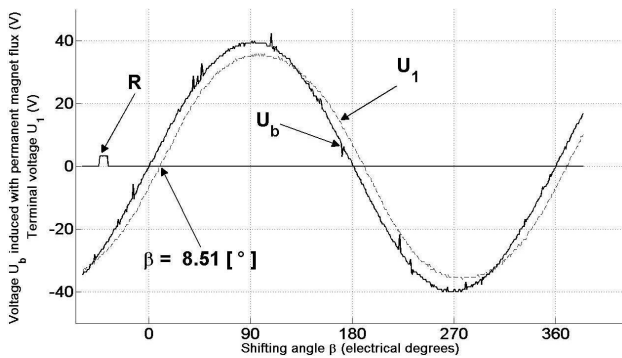


Fig. 7. Shifting angle β between terminal voltage U_1 and voltage U_b induced with permanent magnets. One period of the 8 pole machine.

In the Fig. 7 the position sensor pulse 'R' is written down. Position sensor does not mark the 'd' or 'q' axis with its pulse 'R' but voltage U_b does it. Voltage graph determines in no-load with its zero value the 'd' axis position and with its maximum value the 'q' axis position. The graph U_b is recorded and then the machine is loaded with the resistance at the same velocity. Voltage graph U_1 during full load is recorded too. Both oscillograms (U_b and U_1) were put one on each other with position sensor pulses aligned. Angle between them is angle β .

Using (18) we get for X_q (29) at frequency $f = 52.5$ Hz.

$$X_q = X_{1q} + X_{1\sigma} = \frac{U_1 + R_1 \cdot I_1}{I_1} \cdot \tan \beta, \quad (29)$$

$$X_q = \frac{25.92 + 0.963 \cdot 2.265}{2.265} \cdot \tan(8.51) = 1.856 \Omega.$$

Using (19) we get for L_q (30).

$$L_q = L_{1q} + L_{1\sigma} = \frac{X_{1q} + X_{\sigma 1}}{\omega}, \quad (30)$$

$$L_q = \frac{1.856}{329.87} = 0.005626 \text{ H.}$$

Measured machine has $(L_{1q} + L_{1\sigma}) > (L_{1d} + L_{1\sigma})$ with the ratio:

$$\frac{L_{1q} + L_{1\sigma}}{L_{1d} + L_{1\sigma}} = 1.47.$$

4 EXPERIMENTAL CONFIRMATION OF MEASURED PMSM PARAMETERS

Measured parameters can be used for PMSM characteristics prediction. Let us use the experimentally obtained inductances L_d , L_q and calculate the voltage characteristics of the permanent magnet generator. Let us load the generator with a circuit formed with different impedances $Z_Z = R_Z + j\omega \cdot L_Z$ or $Z_Z = R_Z - j\omega \cdot C_Z$ where the resistance R_Z will be several times changed.

Calculation results are shown in Fig. 8 and Fig. 9.

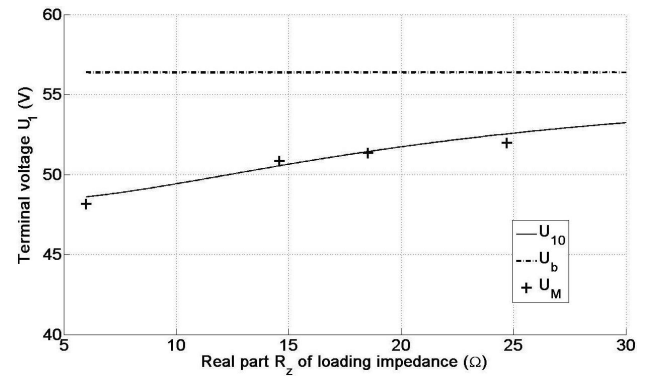


Fig. 8. Calculated voltage characteristic compared with measurement. Three phase symmetrical load is inductive with constant $L_Z = 23.9$ mH and changing resistance R_Z from 6.04 Ω to 30.0 Ω, $f = 101.2$ Hz. Points measured are marked with symbols '+', full line holds for calculated values, dash line holds for no load regime $R_Z \rightarrow \infty$.

Parameters used for calculated characteristics in Fig. 8 are: machine phase resistance $R_1 = 0.963$ Ω machine inductances $L_d = 3.836$ mH and $L_q = 5.626$ mH and frequency $f = 101.2$ Hz. Calculations were performed for symmetrical impedance $Z = R_Z + j\omega \cdot L_Z$. Inductance L_Z was used constant $L_Z = 23.9$ mH while the resistance R_Z has been changed from R_Z from 6.04 Ω to 30.0 Ω. Then the experiment was performed on machine loaded in turn with impedance $Z_Z = R_Z + j\omega \cdot L_Z$ under the same conditions. Inductance L_Z was hold constant $L_Z = 23.9$ mH while the value of resistance R_Z was four times changed $R_Z = 6.0$ Ω; 14.58 Ω; 18.54 Ω; 24.7 Ω. The calculation result is in Fig. 8 compared with measurements. Points measured are marked with symbols '+

Parameters used for calculated characteristics in Fig. 9 are: machine phase resistance $R_d = 0.963$ Ω, machine inductances $L_d = 3.836$ mH, $L_q = 5.626$ mH and frequency $f = 106.6$ Hz. Calculation was performed for

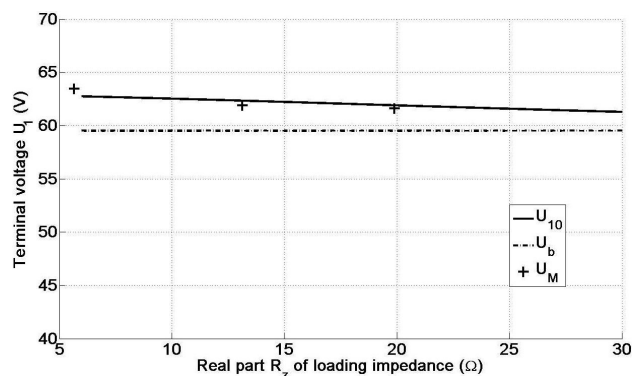


Fig. 9. Calculated voltage characteristic compared with measurement. Three phase symmetrical load is capacitive with constant $C_Z = 0.032$ mF and changing resistance R_Z from 6.00Ω to 30.0Ω , $f = 106.6$ Hz. Points measured are marked with symbols '+', full line holds for calculated values, dash line holds for no load regime $R_Z \rightarrow \infty$.

symmetrical impedance $Z_Z = R_Z - j\frac{1}{\omega C_Z}$. Capacitance C_Z was hold constant $C_Z = 0.032$ mF while the resistance R_Z was changed from R_Z from 6.00Ω to 30.0Ω . Then the machine was loaded in turn with impedance $Z_Z = R_Z - j\frac{1}{\omega C_Z}$ under the same conditions.

Capacitance C_Z was hold constant $C_Z = 0.032$ mF while the value of resistance R_Z was three times changed $R_Z = 5.67 \Omega$; 13.14Ω ; 19.89Ω . The calculation result is in Fig. 9 compared with measurements. Points measured are marked with symbols '+

It can be seen from Fig. 8 and Fig. 9 that the generator inductive current demagnetizes permanent magnets of the generator. The voltage drop is relatively high. The capacitive generator current acts positively with permanent magnet orientation. The outgoing generator voltage is higher then is the voltage in no load.

5 CONCLUSION

Modern electric drives very often use permanent magnet synchronous machines (PMSM). Parameters of these machines influence the drive features. The saliency of PMSM has often high importance for the drive and its control. The saliency is influenced by machine construction and by permanent magnet material quality. Measurement methods for PMSM parameters identification are important. New methods are described in the paper. They are suitable for stator self inductances in direct and quadrature axes identification. They can be used for all construction variation of PMSM and for all permanent magnet materials. Results of measurement methods and their experimental verification are published in the paper. Performed experiments acknowledge the measurement methods.

ACKNOWLEDGMENT

Paper was supported by Josef Božek Research Center of Engine and Automotive Technology at Czech Technical University in Prague.

REFERENCES

- [1] T. Lipo, *Analysis of Synchronous Machines*. Boca Raton, USA: CRC Press, Taylor & Francis Group, 2012.
- [2] H.-O. Seinsch, *Principles of Electric Machinery and Drives*. Stuttgart, Federal Republic of Germany: B.G.Teubner, 1993.
- [3] J. F. Gieras and M. Wing, *Permanent Magnet Motor Technology, Design and Applications*. New York, USA: Marcel Dekker, Inc, 2002.
- [4] L. Novák, J. Novák, and M. Novák, "Electrically driven compressors on turbocharged engines with high speed synchronous motors," in *Proceedings of the 8th Electromotion Conference, EPE*, (Lille, France), pp. 600–605, July 2009.
- [5] Z. Čeřovský, *Commutatorless Variable Speed Synchronous Motor*. Prague, Czech Republic: Academia, 1981.
- [6] Z. Čeřovský, J. Novák, and M. Novák, "High speed synchronous motor control for electrically driven compressors on overcharged gasoline or diesel engines," in *IECON Proceedings (Industrial Electronics Conference)*, (Porto, Portugal), pp. 1162–1167, November 2009.
- [7] Z. Peroutka, "Selected problems of modern ac motor traction drives," in *17th International Conference Electrical Drives and Power Electronics, EDPE11*, (High Tatras, Slovakia), pp. 23–36, September 2011.
- [8] F. De Belie, P. Sergeant, and J. Melkebeek, "A sensorless drive by applying test pulses without affecting the average-current samples," *IEEE Transactions on Power Electronics*, vol. 25, no. 4, pp. 875–888, 2010.
- [9] D. T. Sepsí, P. Stumpf, Z. Varga, R. K. Jordan, and I. Nagy, "Comparative analysis of ICEVs, and different types of EVs," in *ELECTRIMACS'2011*, (Paris, France), p. 6, June 2011.
- [10] M. Jurković and D. Žarko, "Optimized design of a brushless dc permanent magnet motor for propulsion of an ultra light aircraft," *Automatika*, vol. 53, no. 3, pp. 244–254, 2012.
- [11] I. Boldea, M. Paicu, G. Andreescu, and F. Blaabjerg, "Active flux DTFC-SVM sensorless control of IPMSM," *IEEE Transactions on Energy Conversion*, vol. 24, no. 2, pp. 314–322, 2009.
- [12] J. Bauer, S. Flígl, and A. Steimel, "Design and dimensioning of essential passive components for the matrix converter prototype," *Automatika*, vol. 53, no. 3, pp. 225–235, 2012.
- [13] J. Lettl, "Control design of matrix converter system," in *Joint International IEEE Aegean Conference on Electrical Machines and Power Electronics & Electromotion Proceedings*, (Bodrum, Turkey), pp. 480–484, September 2007.

- [14] D. Žarko, D. Ban, and T. A. Lipo, "Analytical calculation of magnetic field distribution in the slotted air gap of a surface permanent-magnet motor using complex relative air-gap permeance," *IEEE Transactions on Magnetics*, vol. 42, no. 7, pp. 1828–1837, 2006.
- [15] B. Cassimere, S. Sudhoff, and D. Sudhoff, "Analytical design model for surface mounted permanent magnet synchronous machines," *IEEE Transactions on Energy Conversion*, vol. 24, no. 2, pp. 347–357, 2009.
- [16] S.-C. Yang and R. Lorenz, "Comparison of resistance-based and inductivity-based self-sensing controls for surface permanent-magnet machines using high-frequency signal injection," *IEEE Transaction on Industry Applications*, vol. 48, no. 3, pp. 977–986, 2012.
- [17] Z. Čerovský and P. Mindl, "Double rotor synchronous generator used as power splitting device in hybrid vehicles," in *Fisita Transactions 2006 and Fisita World Automotive Congress*, (Yokohama, Japan), p. F2006P038T, October 2006.
- [18] R. Helmer, E. Garbe, J. Steinbrink, and B. Ponick, "Combined analytical-numerical calculation of electrical machines," *Acta Technica*, vol. 54, no. 1, pp. 1–18, 2009.
- [19] D. Klumpner, I. Serban, M. Risticvic, and I. Boldea, "Comprehensive experimental analysis of the IPMSM for automotive application," in *12th International Power Electronics and Motion Control Conference EPE-PEMC 2006*, (Portorož, Slovenia), pp. 1776–1783, September 2006.
- [20] K. Kovács and I. Rácz, *Transient phenomena in AC Machines I and II*. Budapest, Hungary: Academy of Science, 1959.



Zdeněk Čerovský was born in Czech Republic Feb. 1, 1930. He graduated from Czech Technical University in Prague. He started his carrier with CKD factory as DC/AC machine designer. He projected hoisting engines, mill stand engines, ship engines, drives for street cars, locos and electric vehicles. He changed for Czechoslovak Academy of Sciences, worked as head of Power Electronics Department in the Institute for Electrical Engineering. Projected the first street car with induction motors in ČSR together with CKD. Received Dr.Sc. degree. Later on was director of the Institute for Electrical Engineering. Changed for Czech Technical University in Prague as Professor. Was visiting professor at the UNI in Hannover Germany. Is member of the Research Center JB of Automotive Technology. He was member of Executive Council of the European Power Electronic Association EPE Brussels and member of EPE-PEMC Council Budapest. He worked in many grants and projects like: Project NATO High Technology No 950918, Grant MPO IMPULS. SATREMA, Grant FI-IM5/171. He works for Italy grant agency. He is emeritus professor at Czech Technical University in Prague.



Miroslav Lev was born in Czech Republic Sept. 20, 1958. He graduated from Czech Technical University in Prague. He graduated from two faculties of the UNI in Prague. He finished at the Faculty of Electrical Engineering the specialization Technical Cybernetics and at the Faculty of Mechanical Engineering the specialization Production Machines and Equipment. He was great deal of his technical activity employed by the Research Institute of Machine Tools and Machining VUOSO, by the factory KONE Lifts and ITI TŮV Group Süddeutschland. At the present time he is employed by Czech Technical University in Prague, Faculty of Electrical Engineering, Department of Electric Drives and Traction. His current interests include mathematical simulation and programming of systems working in real time.

AUTHORS' ADDRESSES

Prof. Zdeněk Čerovský, Dr.Sc.

Miroslav Lev, M.Sc.

Department of Electric Drives and Traction,

Faculty of Electrical Engineering,

Czech Technical University in Prague,

Technická 2, CZ-16627, Prague, Czech Republic

email: cerovsky@fel.cvut.cz, lev@fel.cvut.cz

Received: 2014-03-18

Accepted: 2014-07-04